Aerodynamic Loss Characteristics of a Turbine Blade With Trailing Edge Coolant Ejection: Part 2—External Aerodynamics, Total Pressure Losses, and Predictions

Oguz Uzol

Cengiz Camci

Turbomachinery Heat Transfer Laboratory,
The Pennsylvania State University,
University Park, PA 16802

Investigation of the internal fluid mechanic losses for a turbine blade with trailing edge coolant ejection was present in Uzol et al. (2000). The current study is a detailed experimental investigation of the external subsonic flowfield near the trailing edge and the investigation of the external aerodynamic loss characteristics of the turbine blade with trailing edge coolant ejection system. Particle Image Velocimetry experiments and total pressure surveys in the near wake of the blade are conducted for two different Reynolds numbers and four different ejection rates. Two different trailing edge configurations with different cut-back lengths are also investigated. Numerical simulations of the flowfield are also performed for qualitative flow visualization purposes. Two-dimensional, incompressible, and steady solutions of Reynolds-averaged Navier–Stokes equations are obtained. A two-equation standard k–e turbulence model coupled with an Algebraic Reynolds Stress Model is used for the simulation of the turbulent flowfield. The results show that the aerodynamic penalty levels in the wake region near the trailing edge are increased due to the mixing of the coolant and mainstream flows for 0–3 percent ejection rates. However, after a threshold level (5 percent ejection rate), the ejected coolant flow has enough momentum to fill the wake of the blade, which in turn results in a decrease in the aerodynamic penalty levels. [DOI: 10.1115/1.1351817]

Introduction

In order to increase the specific thrust and to reduce the specific fuel consumption of gas turbine engines, higher turbine inlet temperatures are needed. This need for high temperatures results in a demand for effective cooling of high-pressure turbine blades. Many of the blade cooling systems involve ejection of cooling flows into the hot gas stream at various points on the blade. One of the most critical locations on the blade where coolant ejection is performed is the trailing edge. The mixing of high-density coolant with hot mainstream gases can result in aerodynamic losses, which will influence the engine performance.

Aerodynamic aspects associated with trailing edge coolant ejection in steady two-dimensional blade-to-blade flow over a range of exit Mach numbers and coolant pressure ratios were studied by Deckers and Denton [1]. The tests were carried out on flat plate models representing the region of uncovered turning downstream of the throat. It was concluded that the effect of coolant ejection is a substantial increase in the base pressure and a reduction in overall loss. Pappu and Schobeiri [2] investigated the aerodynamic effects of trailing edge ejection on mixing losses downstream of cooled gas turbine blades. The results indicate that for an ejection velocity ratio of unity, the trailing edge ejection reduces the mixing losses. An investigation of the flow field downstream of a turbine trailing edge cooled nozzle guide van is described in Sieverding et al. [3]. A cutback trailing edge ejection system discharging on the pressure side of the blade is used. It was concluded that the coolant flow ejection did not produce any unusual wake flow patterns in the measurement planes. This feature was explained with very rapid mixing of the coolant with mainstream flow. Mee [4] discussed the experimental methods required to compare different trailing edge region coolant ejection geometries. It is suggested that if the additional complexity associated with foreign gas ejection or cooled air injection is to be avoided, more accurate results may be obtained by simulating the momentum flux ratio rather than the ejection rate of the coolant. Aerodynamic penalties of coolant ejection for two different trailing edge geometries were investigated by Kost and Holmes [5]. A blade with a thick trailing edge where coolant is ejected through slots in the trailing edge and a blade with a thin trailing edge where coolant is ejected through a row of holes on the pressure and suction sides were tested. Their results indicate that for coolant to mainstream mass flow rate ratios larger than 2.5 to 3 percent, the coolant momentum has a positive effect on total loss. Kapteijn et al. [6] tested an inlet guide vane with two different trailing edge shapes to investigate the aerodynamic effects of trailing edge ejection. A fully enclosed trailing edge ejection system and a cut-back trailing edge ejecting on the pressure side were compared. The cut-back trailing edge generates higher losses than the fully enclosed ejection system, especially in the supersonic range.

This study is an extension of the internal loss investigation and discharge coefficient measurements performed by Uzol et al. [7]. The objective is to understand the effect of trailing edge coolant ejection on the external aerodynamic loss characteristics of the turbine blade with the trailing edge coolant ejection system. For this purpose Particle Image Velocimetry (PIV) experiments and total pressure surveys are conducted in the near wake region of the trailing edge. High-resolution flow field maps are obtained for two different Reynolds numbers, namely Re_{max}=500,000 and 350,000, which is calculated using the chord length and the maximum velocity at the throat. The coolant to free-stream mass flow rate ratio, i.e., ejection rate, is varied between 0 and 5 percent. The effect of the trailing edge ejection configuration is also investigated by testing two different cut-back lengths at the trailing edge.

Contributed by the International Gas Turbine Institute and presented at the 45th International Gas Turbine and Aeroengine Congress and Exhibition, Munich, Germany, May 8–11, 2000. Manuscript received by the International Gas Turbine Institute February 2000. Paper No. 2000-GT-557. Review Chair: D. Ballal.

One configuration was a zero cut-back length blade in which the trailing edge ejection occurs right at the trailing edge. The second configuration had a cut-back length of 23 mm (12.5 percent chord) from the trailing edge and the coolant ejection was from the pressure side. Computational simulations of the flowfield are also obtained by solving two-dimensional, incompressible, steady Reynolds-averaged Navier–Stokes equations using a finite element scheme. The numerical results obtained are used for qualitative flow visualization purposes.

Experimental Facility

The experiments are conducted at the ''Cooled Turbine Cascade Facility'' at the Turbomachinery Heat Transfer Laboratory of the Pennsylvania State University. Detailed information about the facility was presented in Uzol et al. [7]

The test section consists of two flow passages that are formed by a linear cascade of three generic high-pressure turbine blade profiles with high trailing edge thickness as explained in Uzol et al. [7] (Fig. 1). The turbine blades have a chord length of 0.1834 m and the pitch is 0.135 m, which gives a pitch-to-chord ratio of 0.736. The blades are placed with a 45 deg stagger angle with an inlet flow angle of 0 deg and an exit flow angle of −76.7 deg. Typical velocity distribution around the airfoil and additional details of the specific cascade can be found in Gangler and Russell [8] and Hippensteele et al. [9]

The middle blade in the cascade is instrumental to simulate trailing edge coolant ejection. The trailing edge is also modified to allow testing of different trailing edge coolant ejection configurations. The geometry and the details of the trailing edge coolant ejection system are explained in detail in Uzol et al. [7]. The specific geometry used in this study has six ribs between the suction side and the pressure side shells, which are enclosed with an aluminum cover plate. The two trailing edge configurations tested

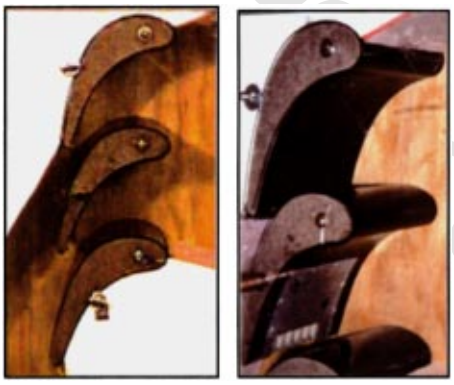

Fig. 1 View of test section

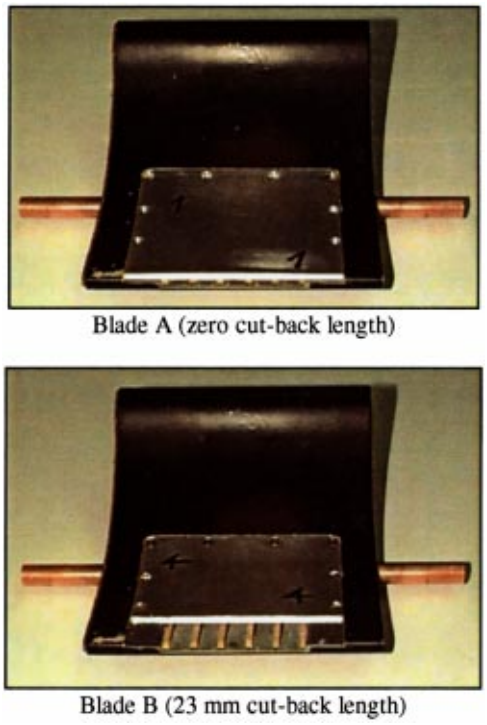

Fig. 2 Trailing edge coolant ejection configurations

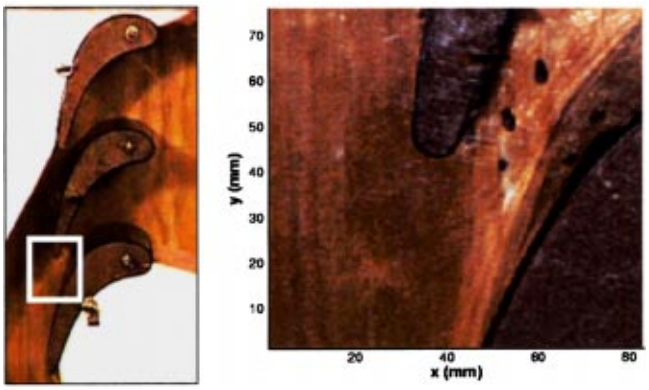

Fig. 3 PIV measurement domain

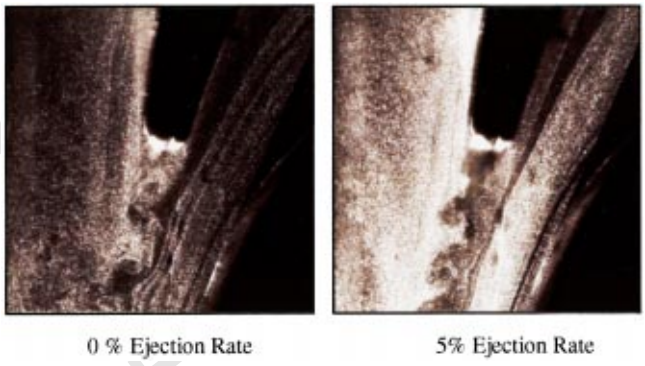

Fig. 4 Typical speckle images for PIV measurements (Blade A)

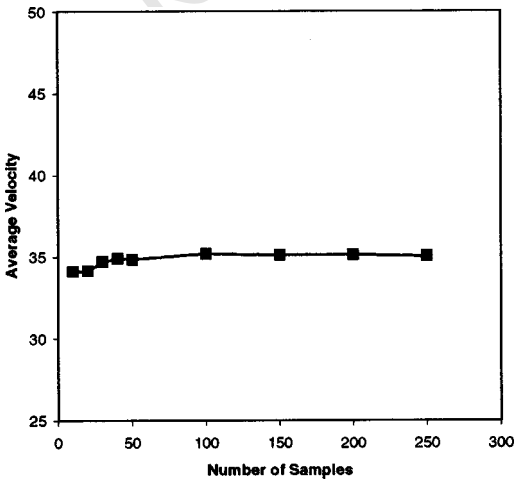

Fig. 5 Variation of the mean velocity inside the wake with number of samples

are a zero cut-back length (Blade A) and a cut-back length of 23 mm on the pressure side (Blade B) (Fig. 2). The blade span is 152.4 mm, which is equal to the endwall to endwall distance in the test section.

Pressurized air is supplied through from both sides of the instrumental blade in order to have a uniform coolant ejection from the trailing edge. The volumetric flow rate of the coolant is controlled by a rotameter. The total pressure and the total temperature of the coolant are also measured just before the coolant goes inside the blade; these measurements are used to calculate the ejection rate. The mainstream flow velocity, total pressure, and total temperature at the inlet of the test section were also measured to obtain the inlet mass flow rate. For a given inlet Reynolds number, the coolant mass flow rate is varied until the desired ejection rate is reached. Once it is reached, 250 PIV speckle images are collected. A miniature total pressure probe mounted on a traverser is also used to measure total pressure losses in addition to velocity field measurements from PIV.

PIV Measurements

Particle Image Velocimetry experiments are conducted for the investigation of the flowfield near the trailing edge of the middle blade (Fig. 1), which was instrumented for creating a coolant ejection from its trailing edge with different trailing edge configurations. The PIV measurement domain is illustrated in Fig. 3.

The flow field is seeded with fog particles and the PIV measurement domain is illuminated by two frequency doubled pulsating Nd:YAG laser sheets, which have an emitted radiation wave-

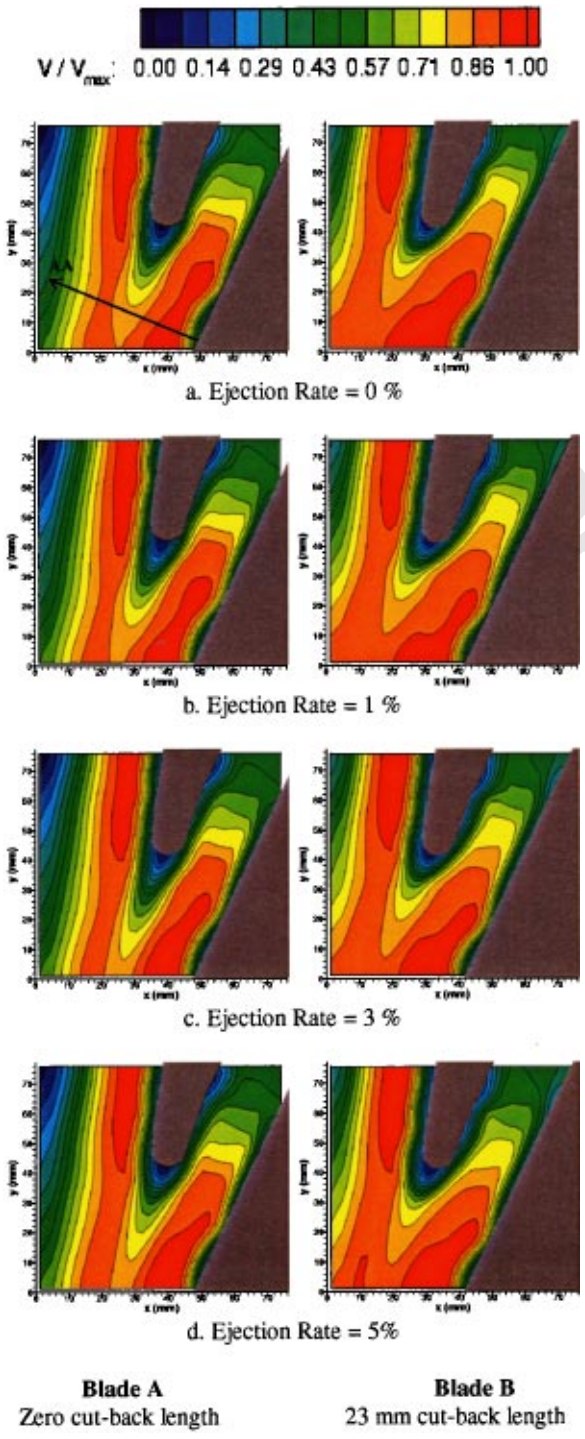

Fig. 6 Measured PIV speed contours at Re_{max}=350.000

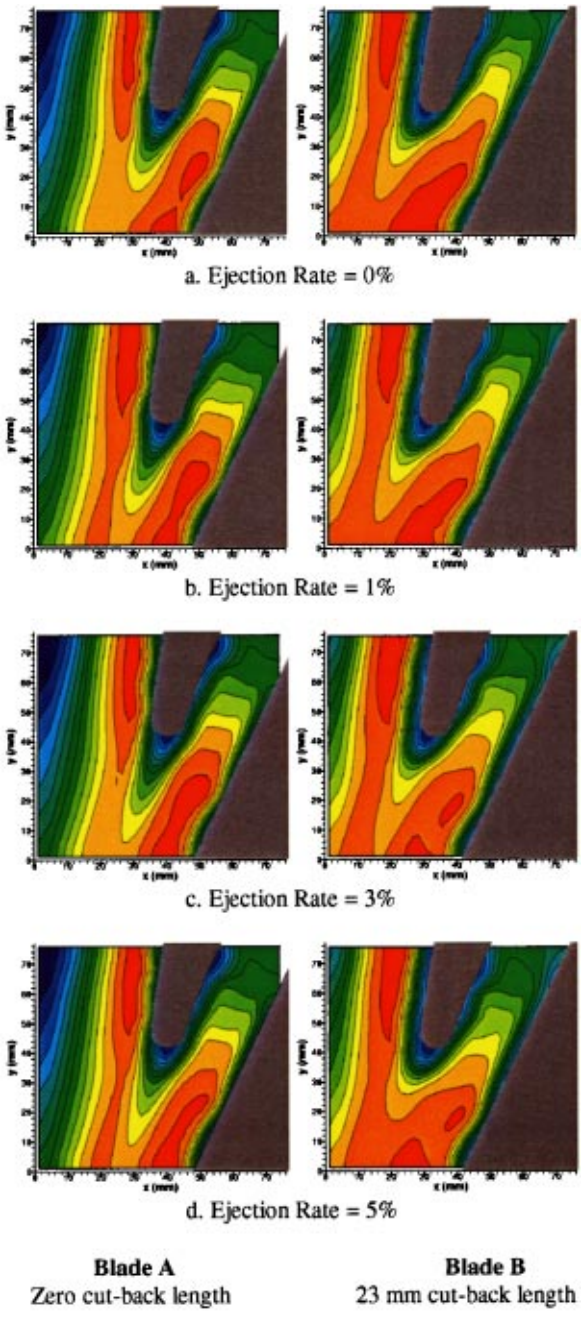

Fig. 7 Measured PIV speed contours at Re_{max}=500,000

length of 532 nm. The pulsed Nd:YAG laser power is 50 mJ and the laser sheet is placed between the third and fourth ribs, which corresponds to the midspan location on the blade. Pairs of speckle images of the PIV domain are then captured using a CCD cross-correlation camera, which is fully synchronized with the pulsating laser sheets. The minimum time delay between the two frames in an image pair that can be obtained in this system is 1 μs. Two different time delay settings of 15 μs and 11 μs are used for two different Re_{max} values of 350,000 and 500,000, respectively. All the synchronization and image-capturing processes are controlled by a DANTEC PIV 2000 processor. The cross-correlation and data reduction processes as well as the control of the PIV 2000 processor are managed by a personal computer. Figure 4 shows typical speckle images of the PIV domain captured with the CCD camera. Although the instantaneous flow details in the wake region in the absence and presence of coolant ejection are illuminated in these images, obtaining information about the unsteady nature of the flow field using these visualizations is beyond the scope of this study. The main purpose is to obtain the true-mean velocity field information, which will be used in the external loss investigation.

For each measurement case (i.e., for a specific combination of Re_{max}, a trailing edge configuration, and an ejection rate), 250 pairs of images are collected. After each pair is cross-correlated

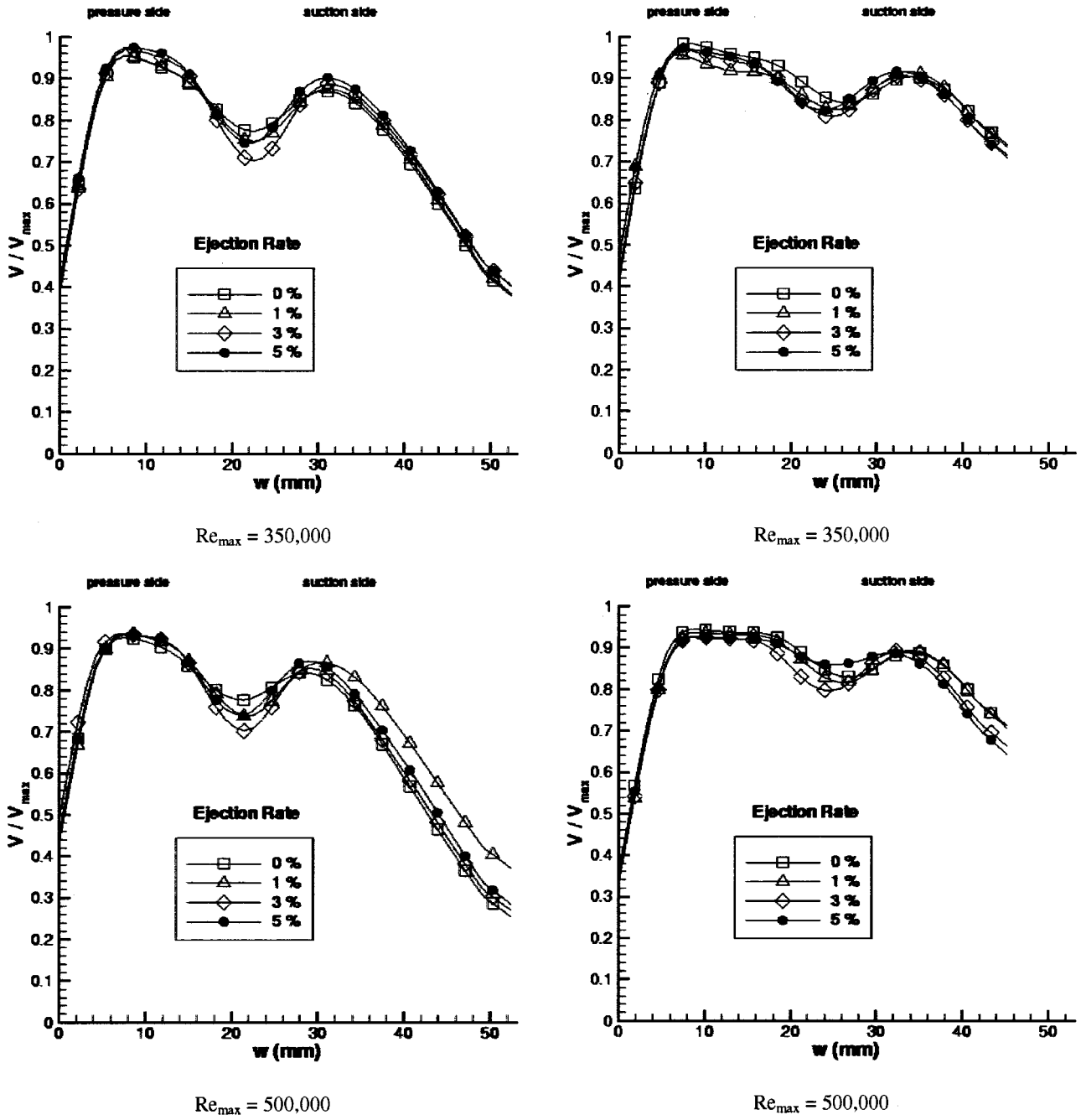

Fig. 8 Measured velocity profiles inside the wake along line *AA*

and the raw velocity fields are moving-averaged/filtered, the mean flow field is obtained by ensemble-averaging over 250 samples. The variation of the mean velocity, which was obtained by taking the average along a certain line (line *AA* in Fig. 6(*a*) inside the wake of the blade, with number of samples is shown in Fig. 5. It is clear that a stationary measurement is obtained after the number of acquired samples exceeds 150. The experimental uncertainty level for the velocity measurements using 250 samples is estimated to be ± 0.5 percent.

Figures 6 and 7 show the speed contours inside the PIV domain for Blades A and B at $Re_{max} = 350{,}000$ and 500,000, respectively. The term speed is used for the magnitude of the velocity vector from PIV measurements throughout this paper. The results are presented for ejection rates of 0, 1, 3, and 5 percent. As can be seen from the plots, it was not possible to obtain physically meaningful data from the right-hand side of the PIV domain because of the blockage of the laser sheet by the trailing edge of the lower blade. That portion of the domain is illustrated as gray triangles in Figs. 6 and 7. The actual laser sheet blockage can be seen in Fig. 4. The rest of the flowfield, however, had sufficient laser illumination, which was used to produce the wake characteristics of the middle blade.

The maximum velocity is reached at the cross section that has the minimum area between the pressure side of the middle blade and the suction side of the lower blade. The quantitative results for the maximum velocity obtained from the PIV measurements are observed to be in close agreement with the data obtained from pitot-static prober measurements acquired at the minimum area plane, as explained in Uzol et al. [7]. It is also observed that there is no separation on the suction side of the middle blade for both Reynolds numbers and both trailing edge configurations. The suction side boundary layer stays attached and mixes with the pressure side boundary layer at the trailing edge. This mixing of the suction and pressure side wall shear layers create an almost symmetric low-momentum field, in the region close to the trailing edge of Blade A (zero cut-back length). The small asymmetry that still exists is due to the difference in the thickness of these boundary layers. The near-wake region of Blade B, however, shows a greater asymmetry, which can easily be depicted in Fig. 6. This is mainly due to the effect of the cut-back region, which behaves as a backward-facing step and modifies the boundary layer behavior on the pressure side. The existence of the cut-back region diverts the speed contours toward the suction side at the trailing edge.

As the ejection rate is increased from 0 to 5 percent, some changes in the wake patters occur. For both trailing edge configuration, the low-momentum region extends more and more as the ejection rate is increased from 0 to 3 percent. However, for 5 percent coolant ejection, the low-momentum region becomes smaller. This behavior of the wake pattern is evident in Fig. 8 in which the velocity profiles inside the wake along line *AA* (Fig. 6(*a*)) are illustrated. For both Reynolds numbers and trailing edge configurations, the velocity defect in the velocity profile becomes more significant up to 3 percent ejection rate. However, again for all cases, a decrease of the velocity defect inside the wake is observed for 5 percent coolant ejection. This particular variation of the wake patterns with varying ejection rates will have a significant effect on the blade total pressure loss characteristics.

Effect of Cut-Back Length

The effect of the cut-back length is illustrated in Fig. 9, which shows the velocity profiles along line *AA* for blades A and B, at a free-stream Reynolds number of 500,000 and for a 0 percent ejection rate. A shift in the position of the velocity defect in the velocity profile inside the wake can be observed from this figure. The minimum velocity region is shifted toward the suction side for Blade B. Although the results shown are for 0 percent ejection rate, the same shift pattern is also observed for all the other ejection rates. This shift in the velocity defect is mainly due to the reason that the pressure side shell is not complete for Blade B.

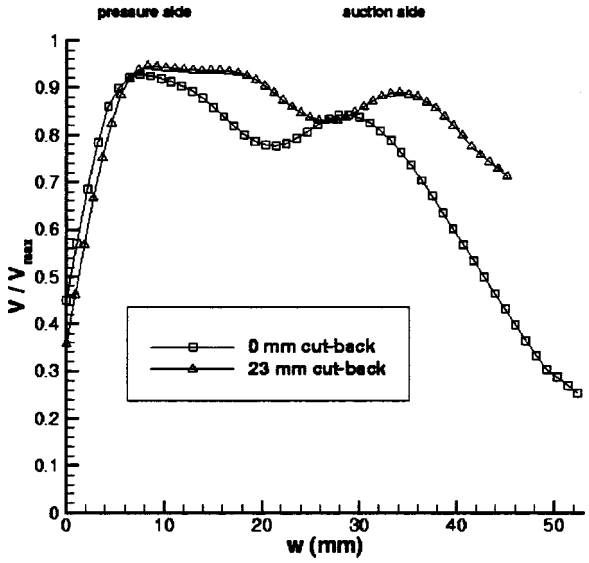

Fig. 9 Effect of cut-back length on wake velocity defect (0 percent ejection rate)

Therefore, in the near-wake region the velocity defect for Blade B is just because of the suction side shell, which clearly has a smaller defect because of the smaller thickness at the trailing edge.

Total Pressure Loss Measurements

As a complementary study for the PIV measurements, a total pressure traverse inside the near wake of the middle blade, again along line *AA*, is performed independently using a total pressure probe. The uncertainty level for the pressure measurements is estimated to be ± 0.5 percent at 105,000 N/m^2 (typical atmospheric value). The results are shown in Fig. 10, and show similar wake characteristics to the PIV results. The total pressure loss levels increase with increasing ejection rate up to 3 percent, and at 5 percent coolant ejection the losses are minimized. Furthermore, at 5 percent ejection the local total pressure increase due to the high-momentum coolant jet ejection can be seen in Fig. 9. Consequently, both the PIV results and the total pressure traverse results show that the coolant ejection has a negative effect, in terms of total pressure losses, until a certain ejection rate is reached. This behavior was also observed by previous researchers. Kost and Holmes [5] indicate that for coolant to mainstream mass flow rate ratios larger than 2.5 to 3 percent, the coolant momentum has a positive effect on total loss, both for pressure side coolant ejection and for the ejection from a slot at the trailing edge. Their results are for a cascade operating at an exit Mach number of 0.76, which is below the design condition. It is concluded that by ejecting a moderate amount of coolant from a row of holes into subsonic local flow, a decrease of profile loss will be achieved if the coolant momentum has a component in the main flow direction. Pappu and Schobeiri [2] also indicate that increasing the coolant to mainstream velocity ratio yields a deeper wake in comparison to the no-injection case and consequently in higher total pressure losses for a turbine blade trailing edge coolant ejection system without a cut-back length. The main physical reason for this phenomenon is explained thus: The ejected coolant jet does not have enough momentum to overcome the strong dissipative nature of the wake at the trailing edge, which results in the dissipation of the kinetic energy of the jet. This dissipation yields a deeper wake than for the no-injection case. The aerothermodynamic modeling and performance analysis of Kim et al. [10] for a turbine stage having cooled nozzle blades also show that ejection of coolant causes total pressure losses up to 2–3 percent of the ejection rate. How-

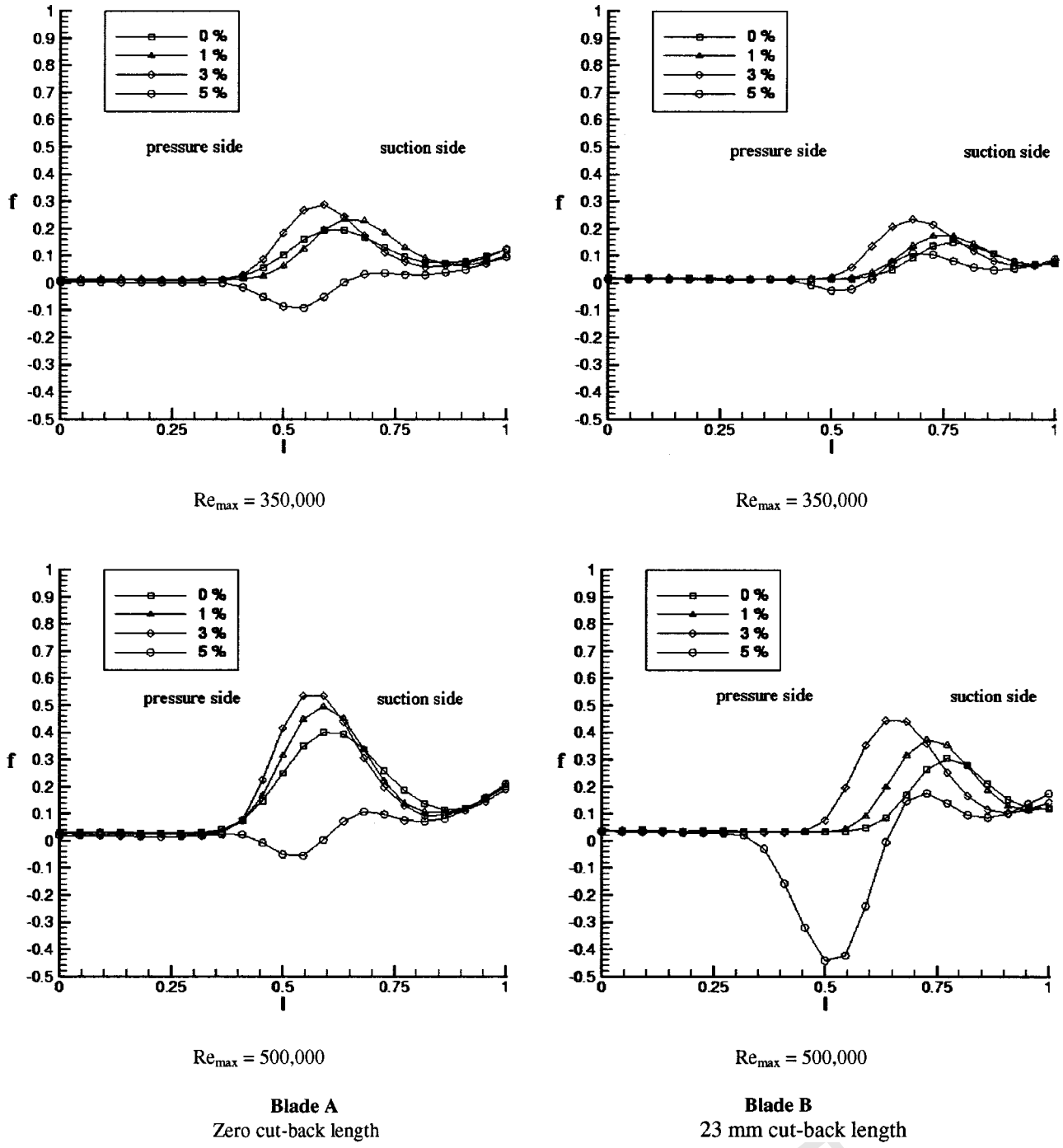

Fig. 10 Measured total pressure loss profiles along line *AA*

ever, when the momentum contribution of the $Re_{max}=500{,}000$ coolant becomes significant, a total pressure gain is predicted when compared to the no-injection case.

The main reason for this increase in loss for low ejection rates is that the ejected coolant has a very low momentum when compared to the mainstream flow. Therefore, when the low-momentum coolant jet mixes with the high-momentum mainstream, mixing losses are created by high shear regions, which cause increases in the turbulence production in these regions. Hence, some part of the kinetic energy of the main flow is wasted through this turbulence production mechanism and this reflects as an increase in the total pressure loss levels in the wake. However, for high ejection rates like 5 percent, the ejected coolant jet has comparable momentum with the mainstream and it fills the low-momentum region inside the wake, yielding lower loss levels. This kind of behavior of the loss mechanism is observed for both trailing edge configurations and Reynolds numbers.

The total pressure loss levels for Blade B, which has a 23 mm cut-back length, are also observed to be less than that of Blade A, which has a zero cut-back length. This is due to the fact that the low-momentum region inside the wake coming from the pressure side wall shear layer of Blade A (zero cut-back length) is filled with the momentum of the coolant jet in case of Blade B. Even when there is no ejection, this region is again filled with the momentum of the mainstream coming over the back-step region. Hence this results in a reduction in the total pressure loss levels for Blade B (23 mm cut-back length).

Computational Simulations

Solutions of the two-dimensional, steady, and incompressible Reynolds-averaged Navier–Stokes equations are obtained for the test section geometry using a finite element methodology. These results are basically used for qualitative flow visualization of the flow field. A standard $k-e$ turbulence model coupled with Lander's [11] Algebraic Reynolds Stress Model is used for the simulation of the turbulent flow field. The governing equations for the flow field are:

$$u_{i,i}^* = 0 \tag{1}$$

$$\frac{\partial u_i^*}{\partial t} + u_j^* u_{i,j}^* = -p_{,i}^* + \frac{1}{\mathrm{Re}}[\mu^*(u_{i,j}^* + u_{j,i}^*)]_j \tag{2}$$

$$\frac{\partial k^*}{\partial t^*} + u_j^* k_{,j}^* = \left(\frac{\mu_t^*}{\sigma_k} k_{,j}^*\right)_j - \varepsilon^* + \mu_t^* \Phi^* \tag{3}$$

$$\frac{\partial \varepsilon^*}{\partial t^*} + u_j^* \varepsilon_{,j}^* = \left(\frac{\mu_t^*}{\sigma_k} \varepsilon_{,j}^*\right)_{,j} + C_1 \left(\frac{\varepsilon^*}{k^*}\right) \mu_t^* \Phi^* - c_2 \frac{\varepsilon^{*2}}{k^*} \tag{4}$$

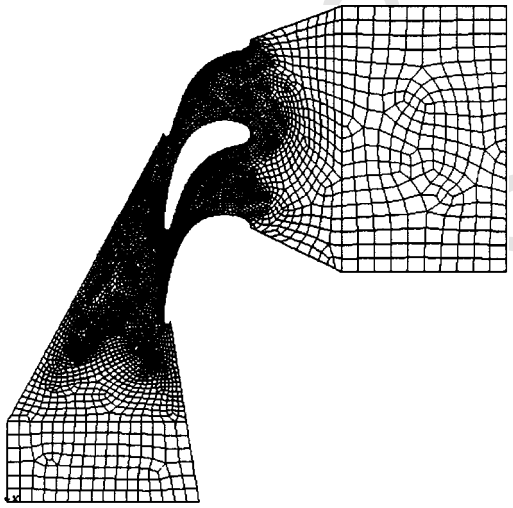

Blade A

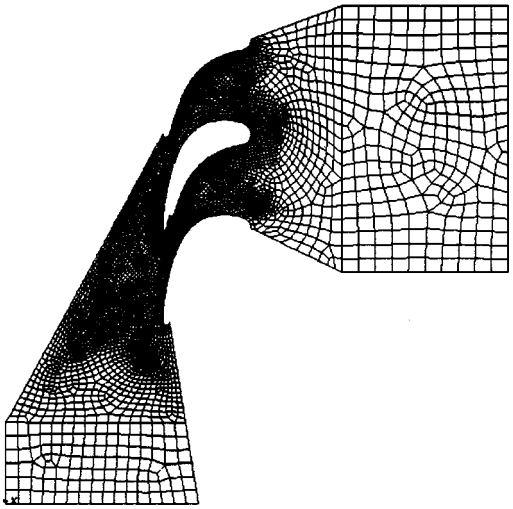

Blade B

Fig. 11 Computational meshes for Blades A and B

A finite element-based fluid dynamics analysis package, FIDAP [12], is used to solve the governing equations. The flow domain is discretized by using nine-node quadrilateral elements, which give a biquadratic velocity and bilinear pressure variation within each element. Velocity components are specified as zero on the walls and on the blade in order to satisfy the no-slip condition. At the inlet of the test section, the x component of the velocity is specified as a uniform steady profile and the y component is specified as zero. At the trailing edge of the blade, the coolant ejection velocity is specified as a uniform profile that corresponds to the desired coolant ejection rate. Values for the turbulent kinetic energy and for the dissipation rate of turbulent kinetic energy corre-

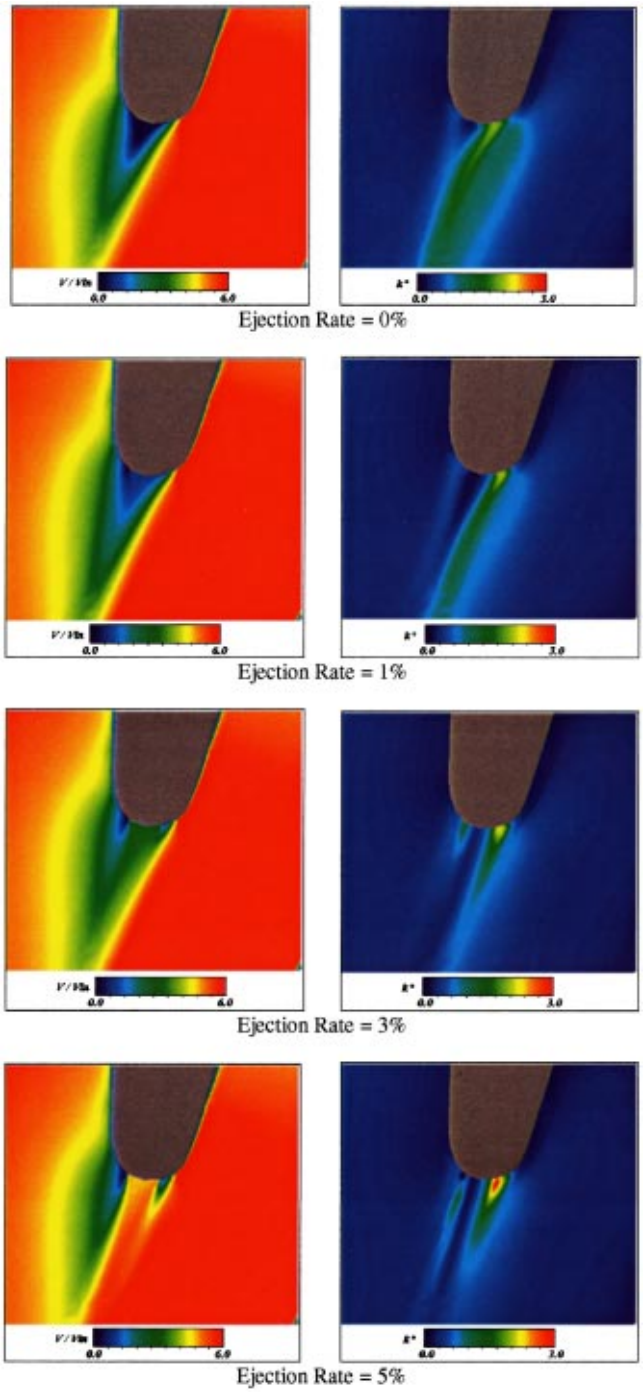

Fig. 12 Speed contours and turbulent kinetic energy contours for Blade A

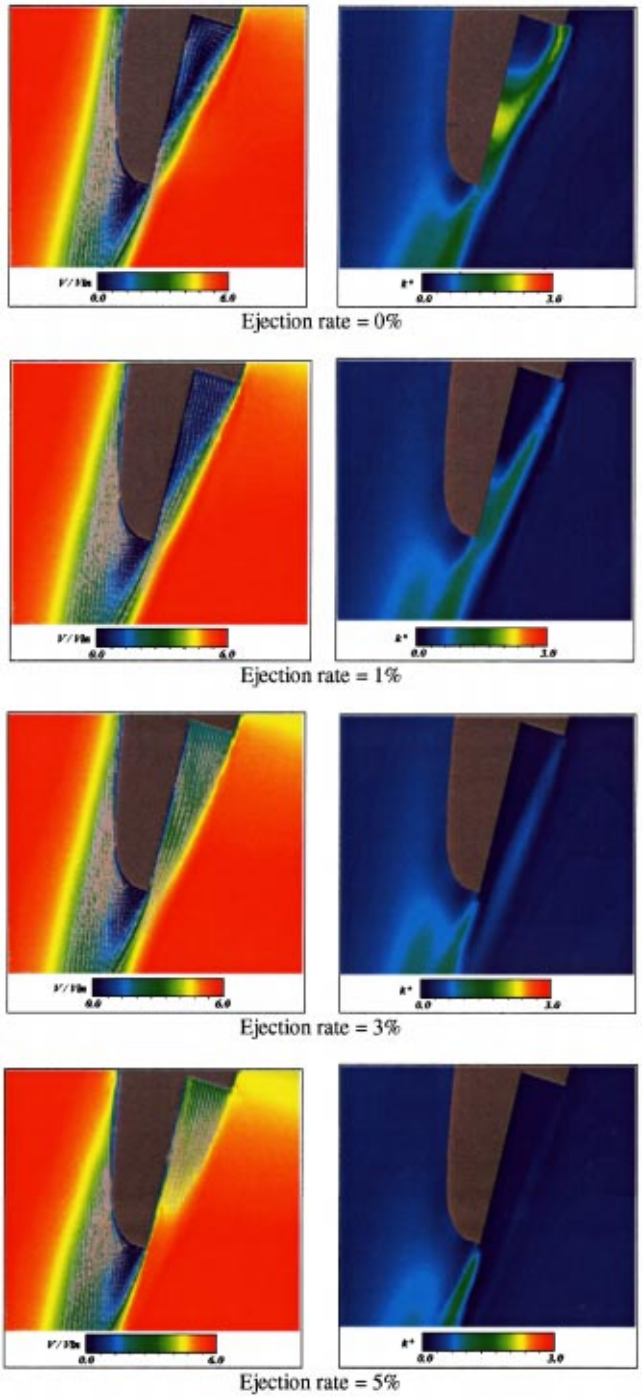

Fig. 13 Speed contours and turbulent kinetic energy contours for Blade B

sponding to a 1.2 percent turbulence intensity level are also specified at the test section inlet. This level of turbulence intensity is obtained from single sensor hot-wire measurements at that location. For the Blade A case, 6640 second-order finite elements are created, which resulted in 24,776 nodes. For Blade B, 6555 second-order elements are used, which gives 24442 nodes. The computational meshes used for Blade A and B are illustrated in Fig. 11.

Figures 12 and 13 illustrate the results of the computational analysis near the trailing edges of Blades A and B, respectively. The speed contours and the turbulent kinetic energy distribution of the flow field are shown in these figures. The recirculatory region inside the cut-back length of Blade B is clearly seen in Fig. 13 for 0 percent ejection rate. As the ejection rate is increased, this region vanishes, and the coolant ejection starts to dominate the cut-back region on the trailing edge. The formation of this strong recirculatory region at low ejection rates is the main reason for the increase in losses, which in turn result in low discharge coefficients for a trailing edge with along enough cut-back length [7]. As can be seen from the turbulent kinetic energy plots, the turbulent kinetic energy production inside the high shear regions is high for 0 and 1 percent ejection rates when compared to the higher ejection rates. However, as the ejection rate increases, the turbulent kinetic energy generation goes down because of the reduction of the shear between the ejected coolant and the main flow. This behavior is closely related to the total pressure loss characteristics of the blade because it is the shear between the coolant and the mainstream that determines the kinetic energy losses. These in turn result in the creation of total pressure losses inside wake as observed from PIV and total pressure loss measurements.

Conclusions

The subsonic external flow field physics near the trailing edge of a turbine blade with a coolant ejection system is investigated in order to determine the external aerodynamic loss behavior of the blade due to trailing edge coolant ejection for different ejection rates. Particle Image Velocimetry (PIV) and total pressure loss measurement results show that the mixing of the coolant flow with the mainstream result in an increase in loss levels for 0–3 percent ejection rates. However, when the coolant ejection rate reaches 5 percent, the loss levels are minimized and even local total pressure increases are observed due to the high-momentum coolant jet. This behavior of the loss mechanism is observed both for the blade with a zero cut-backlength and for the blade with a 23 mm cut-back length at the trailing edge. The main possible reason for this kind of behavior at low ejection rates is the creation of mixing losses due to the mixing of high-momentum mainstream and the low-momentum coolant flow. The effect of the cut-back length was determined to be a shift in the velocity defect region in the wake velocity profile. Additionally, the blade with the cut-back length at the trailing edge is observed to have a smaller velocity defect in the profile that will lead to less aerodynamic loss. The results of the computational simulations reveal the existence of a recirculatory region inside the cut-back length of Blade B for 0 percent ejection, which results in a reduction in the discharge coefficient values for this specific trailing edge arrangement. the turbulence generation is also numerically visualized as the ejection rate is changed from 0 to 5 percent. It is observed that the behavior of the shear generated between the mainstream and the coolant flow mainly determines most of the loss characteristics of the blade. Numerical simulation results illuminate the details of the flow field that could not be captured by PIV.

Acknowledgments

The turbine cascade used in the current study was provided by NASA Lewis (Glenn) Research Center. The authors would like to acknowledge the equipment support provided by S. A. Hippensteele and Dr. R. E. Gaugler of NASA (Glenn) Research Center, Cleveland, Ohio. The authors are also grateful for the equipment grant provided by the College of Engineering of the Pennsylvania State University. The grant was used for the acquisition of the PIV equipment extensively used in this study.

Nomenclature

f = total pressure loss coefficient $=(P_{tin}-P_{tex})/P_{tin}\times 100$
k = turbulent kinetic energy
k^* = k/u_0^2=nondimensional turbulent kinetic energy
l = $w/w_{\max}$=nondimensional total pressure traverse distance parameter

p = static pressure
p^* = $(p-p_{\text{ref}})/\rho u_0^2$=nondimensional static pressure
$\text{Re}_{\max}$ = maximum Reynolds number calculated using maximum velocity at throat and blade chord
u_i = ith component of velocity vector
u_i^* = u_i/u_0=nondimensional velocity
V = magnitude of velocity vector
V_{in} = velocity at inlet of test section
$V_{\max}$ = maximum velocity at throat
w = distance parameter along line AA, mm
$w_{\max}$ = maximum distance on AA, mm
x_i = ith component of spatial coordinate
x_i^* = x_i/D=nondimensional coordinate
ε = viscous dissipation rate of turbulent kinetic energy
ε^* = $\varepsilon D/u_0^3$=nondimensional viscous dissipation rate of turbulent kinetic energy
Φ = viscous dissipation function
Φ^* = $\Phi D^2/u_0^2$=nondimensional viscous dissipation function
μ_0 = absolute viscosity
μ_t = turbulent viscosity
μ_t^* = $\mu_t/(\rho u_0/D)$=nondimensional turbulent viscosity
μ^* = $1+\mu_t/\mu_0$=nondimensional viscosity
ρ = density

References

[1] Deckers, M., and Denton, J. D., 1997, ''The Aerodynamics of Trailing-Edge-Cooled Transonic Turbine Blades: Part 1—Experimental Approach,'' ASME Paper No. 97-FT-518.

[2] Pappu, K. R., and Schobeiri, M. T., 1997, ''Optimization of Trailing Edge Ejection Mixing Losses: A Theoretical and Experimental Study,'' ASME Paper No. 97-GT-523.

[3] Sieverding, C. H., Arts, T., Dénos, R., and Martelli, F., 1996, ''Investigation of the Flow Field Downstream of a Turbine Trailing Edge Cooled Nozzle Guide Vane,'' ASME J. Turbomach., **118**, pp. 291–300.

[4] Mee, D. J., 1992, '''Techniques for Aerodynamic Loss Measurement of Transonic Turbine Cascades With Trailing-Edge Region Coolant Ejection,'' ASME Paper No. 92-GT-157.

[5] Kost, F. H., and Holmes, A. T., 1985, ''Aerodynamic Effect of Coolant Ejection in the Rear Part of Transonic Rotor Blades,'' in: *Heat Transfer and Cooling in Gas Turbines*, AGARD Conference Proceedings No. 390, pp. 41-1–41-12.

[6] Kapteijn, C., Amecke, J., and Michelassi, V., 1996, ''Aerodynamic Performance of a Transonic Turbine Guide Vane With Trailing Edge Coolant Ejection: Part 1:—Experimental Approach,'' ASME J. Turbomach., **118**, pp. 519–528.

[7] Uzol, O., Camci, C., and Glezer, B., 2001, ''Aerodynamic Loss Characteristics of a Turbine Blade With Trailing Edge Coolant Ejection: Part 1—Effect of Cut-Back Length, Spanwise Rib Spacing, Free-Stream Reynolds Number, and Chordwise Rib Length on Discharge Coefficients,'' ASME J. Turbomach., **123**, pp. ■■■–■■■.

[8] Gaugler, R. E., and Russell, L. M., 1980, ''Streakline Flow Visualization Study of a Horseshoe Vortex in a Large-Scale, Two-Dimensional Turbine Stator Cascade,'' ASME Paper No. 80-GT-4.

[9] Hippensteele, S. A., Russell, L. M., and Torres, F. J., 1995, ''Local Heat Transfer Measurements on a Large, Scale-Model Turbine Blade Airfoil Using a Composite of a Heater Element and Liquid Crystals,'' NASA TM 86900.

[10] Kim, J. H., Kim, T. S., Lee, J. S., and Ro, S. T., 1996, ''Performance Analysis of a Turbine Stage Having Cooled Nozzle Blades With Trailing Edge Ejection,'' ASME Paper No. 96-TA-12.

[11] Launder, B. E., 1993, ''Lecture Notes on Turbulence Modeling in Industrial Flows,'' Les Houches Summer School on Computational Fluid Dynamics; also in FIDAP, 1993.

[12] Fluid Dynamics International, Inc., 1993, FIDAP 7.0 Users' Manual.